Hindawi Publishing Corporation
Journal of Nanomaterials
Volume 2015, Article ID 519303, 6 pages
http://dx.doi.org/10.1155/2015/519303

Research Article

Microbe-Assisted Synthesis and Luminescence Properties of Monodispersed Tb^{3+}-Doped ZnS Nanocrystals

Zhanguo Liang,[1] Jun Mu,[1,2] Lei Han,[1] and Hongquan Yu[1]

[1]*School of Environmental and Chemical Engineering, Dalian Jiaotong University, 794 Huanghe Road, Shahekou District, Dalian, Liaoning 116028, China*
[2]*College of Marine Science and Technology, Zhejiang Ocean University, 1 Hadananlu Changshidao Lincheng, Zhoushan, Zhejiang 316022, China*

Correspondence should be addressed to Jun Mu; 2240254374@qq.com

Received 29 August 2014; Accepted 19 October 2014

Academic Editor: Songjun Zeng

Tb^{3+}-doped zinc sulfide (ZnS:Tb^{3+}) nanocrystals were synthesized by spray precipitation with sulfate-reducing bacterial (SRB) culture at room temperature. The morphology of the SRB and ZnS:Tb^{3+} nanocrystals was examined by scanning electron microscopy, and the ZnS:Tb^{3+} nanocrystals were characterized by X-ray diffractometry and photoluminescence (PL) spectroscopy. The PL mechanism of ZnS:Tb^{3+} nanocrystals was further analyzed, and the effects of Tb^{3+} ion concentration on the luminescence properties of ZnS:Tb^{3+} nanocrystals were studied. ZnS:Tb^{3+} nanocrystals showed a sphalerite phase, and the prepared ZnS:Tb^{3+} nanocrystals had high luminescence intensity under excitation at 369 nm. The main peak position of the absorption spectra positively blueshifted with increasing concentrations of Tb^{3+} dopant. Based on the strength of the peak of the excitation and emission spectra, we inferred that the optimum concentration of the Tb^{3+} dopant is 5 mol%. Four main emission peaks were obtained under excitation at 369 nm:489 nm ($^5D_4 \rightarrow {}^7F_6$), 545 nm ($^5D_4 \rightarrow {}^7F_5$), 594 nm ($^5D_4 \rightarrow {}^7F_4$), and 625 nm ($^5D_4 \rightarrow {}^7F_3$). Our findings suggest that nanocrystals have potential applications in photoelectronic devices and biomarkers.

1. Introduction

Zinc sulfide (ZnS) is one of the most important II–IV semiconductors with a band gap of approximately 3.6 eV [1] and is commercially used as a phosphor and thin film in electroluminescent devices. ZnS has been investigated over a period of 20 years as the host material of phosphor layers of electroluminescent devices and field emission displays. ZnS phosphor layers containing transition metal or rare earth metal elements as luminescent centers have been deposited using sputter deposition, thermal evaporation, and electron beam evaporation [2]. Rare-earth-doped wide-band-gap semiconductors have attracted considerable interest in recent years because of attempts to develop novel optoelectronic devices, which combine the unique luminescence features of rare earth ions [3–5]. Since Bhargava et al. first reported the remarkable optical properties of Mn-doped ZnS nanocrystals prepared by chemical process at room temperature in 1994 [6, 7], a large number of investigations on semiconductor nanocrystals have focused on the photoluminescence properties of Mn-doped ZnS nanocrystals [8–16], Cu-doped ZnS nanocrystals [9, 17], Sm-doped ZnS nanocrystals [18], Tb-doped ZnS nanocrystals [18–20], and Eu-doped ZnS nanocrystals [21–25] prepared by different techniques [26]. These papers, however, do not report on ZnS:Tb^{3+} nanocrystals synthesized by spray precipitation method in sulfate-reducing bacterial (SRB) culture at room temperature.

The synthesis process of ZnS:Tb^{3+} nanocrystals is a two-pronged process: one phase involves prepreparation of the sulfur source and capping agent by SRB and the other phase involves synthesis of ZnS:Tb^{3+} nanocrystals by spray precipitation. The first phase shows high efficiency in reducing hexavalent or tetravalent sulfur ions to divalent sulfur ions, which are then effectively fixed in the form of precipitates in the second phase. Thus, reduction of the content of organic pollutants and sulfur in wastewater and synthesis of luminescent nanomaterials under lower energy consumption

Table 1: Molar ratios of Tb^{3+} and Zn^{2+} in $Tb_xZn_{1-x}S$.

	$Tb_xZn_{1-x}S$	$Tb_xZn_{1-x}S$	$Tb_xZn_{1-x}S$	$Tb_xZn_{1-x}S$	$Tb_xZn_{1-x}S$	$Tb_xZn_{1-x}S$
Tb^{3+}	0	0.01	0.03	0.05	0.07	0.09
Zn^{2+}	1.0	0.99	0.97	0.95	0.93	0.91

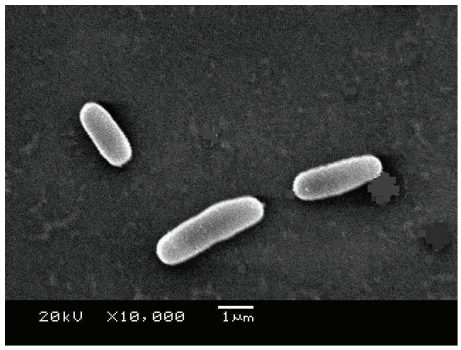

Figure 1: SEM image of the SRB.

may simultaneously be achieved. We have also developed a spray precipitation method based on the conventional precipitation method. ZnS:Tb^{3+} nanocrystals prepared by spray precipitation are smaller and more uniform than those prepared by direct precipitation. The defect of direct precipitation is that its resultant nanoparticles are either too large or highly uneven in size. The spray precipitation method avoids this defect of direct precipitation. Thus, the proposed method may be promoted for the treatment of wastewater with high sulfur contents and the preparation of nanoscale materials.

In this work, the morphology, phase structure, and luminescence properties of ZnS:Tb^{3+} nanocrystals prepared by spray precipitation with different Tb^{3+} doping concentrations were studied.

2. Experiments

2.1. Prepreparation of Sulfur Source and Capping Agent. The SRB was isolated from seawater samples obtained from Heishijiao in Dalian, China. The morphology of the SRB is shown in Figure 1. The scanning electron microscopy (SEM) image in this figure shows that the SRB are a type of short-rod bacteria. The basal culture broth contained 0.5 g L^{-1} KH_2PO_4, 1.0 g L^{-1} NH_4Cl, 1.0 g L^{-1} Na_2SO_4, 2.0 g L^{-1} $MgSO_4{\cdot}7H_2O$, 5.0 g L^{-1} 70% sodium lactate, 0.1 g L^{-1} $CaCl_2{\cdot}2H_2O$, 0.5 g L^{-1} $FeSO_4{\cdot}7H_2O$, 0.1 g L^{-1} sodium thioglycolate, and 0.1 g L^{-1} vitamin C (pH 7.2).

SRB cultivation was performed in sealed glass bottles (125 mL) at 28°C for 3 wk with 5% (v/v) inoculum amount. The SO_4^{2-} in the system was gradually reduced to S^{2-} during cultivation, producing a variety of amino acids (see (1)).

Metabolic products of the bacteria were harvested from the fermentate by centrifugation for 6 min at 10,000 r/min. S^{2-} and a variety of amino acids in the metabolic products were, respectively, used as the sulfur source and the synthesis capping agent:

$$SO_4^{2-} \longrightarrow S^{2-} \quad (1)$$

$$S^{2-} + Zn^{2+} + Tb^{3+} \longrightarrow Tb_xZn_{1-x}S \quad (2)$$

2.2. Synthesis. ZnS:Tb^{3+} nanocrystals were prepared by spray precipitation using S^{2-} and a variety of amino acids obtained from the metabolic products as the sulfur source and the synthesis capping agent, respectively (see (2)).

Zinc acetate and terbium chloride hexahydrate with different molar ratios were dissolved in 100 mL of deionized water (see Table 1). Subsequently, 100 mL of the homogeneous solution was sprayed as fog particles on the surface of metabolic products with S^{2-} and a variety of amino acids. This procedure successfully yielded monodispersed ZnS:Tb^{3+} nanoparticles with different molar ratios at room temperature. The products were then washed three times with deionized water and ethanol and dried in a thermostatic vacuum drier. We prepared a large number of ZnS:Tb^{3+} nanoparticles with particle sizes of 80 nm and then studied the luminescence properties of these particles.

2.3. Characterization. The nanocrystal size and morphology of the samples were observed by using a scanning electron microscope (SEM, JSM-6360LV, JEOL, Japan) and a transmission electron microscope (TEM, JOEL-2100F, JEOL, Japan). Crystal structures were characterized by an X-ray power diffractometer (XRD) using a Netherlands Empyrean diffractometer with Cu$K\alpha_1$ radiation (λ = 0.1541 nm). UV-Vis absorption spectra (absorption wavelength range and maximum absorption wavelength) were obtained by using a V-550 ultraviolet spectrophotometer (JASCO Corp.). Photoluminescence (PL) spectra were measured using a Hitachi F-4500 fluorescence spectrometer.

3. Results and Discussions

ZnS:Tb^{3+} nanocrystals were synthesized by the direct precipitation and spray precipitation methods with SRB culture (Figures 2(a), 2(b), 2(c), 2(d), 2(e), 2(f), and 2(g)). ZnS:Tb^{3+} nanocrystals synthesized by direct precipitation agglomerated and formed large particles, whereas ZnS:Tb^{3+} nanocrystals synthesized by spray precipitation formed homogeneous first agglomeration spherical particles approximately 80 nm in diameter. Only slight second agglomeration was observed among spray-precipitated nanocrystals. From the TEM image of ZnS:Tb^{3+} nanocrystals, we may know that the most initial nanocrystals were approximately 10 nm in diameter (shown in Figure 2(g)). Agglomeration is attributed to two

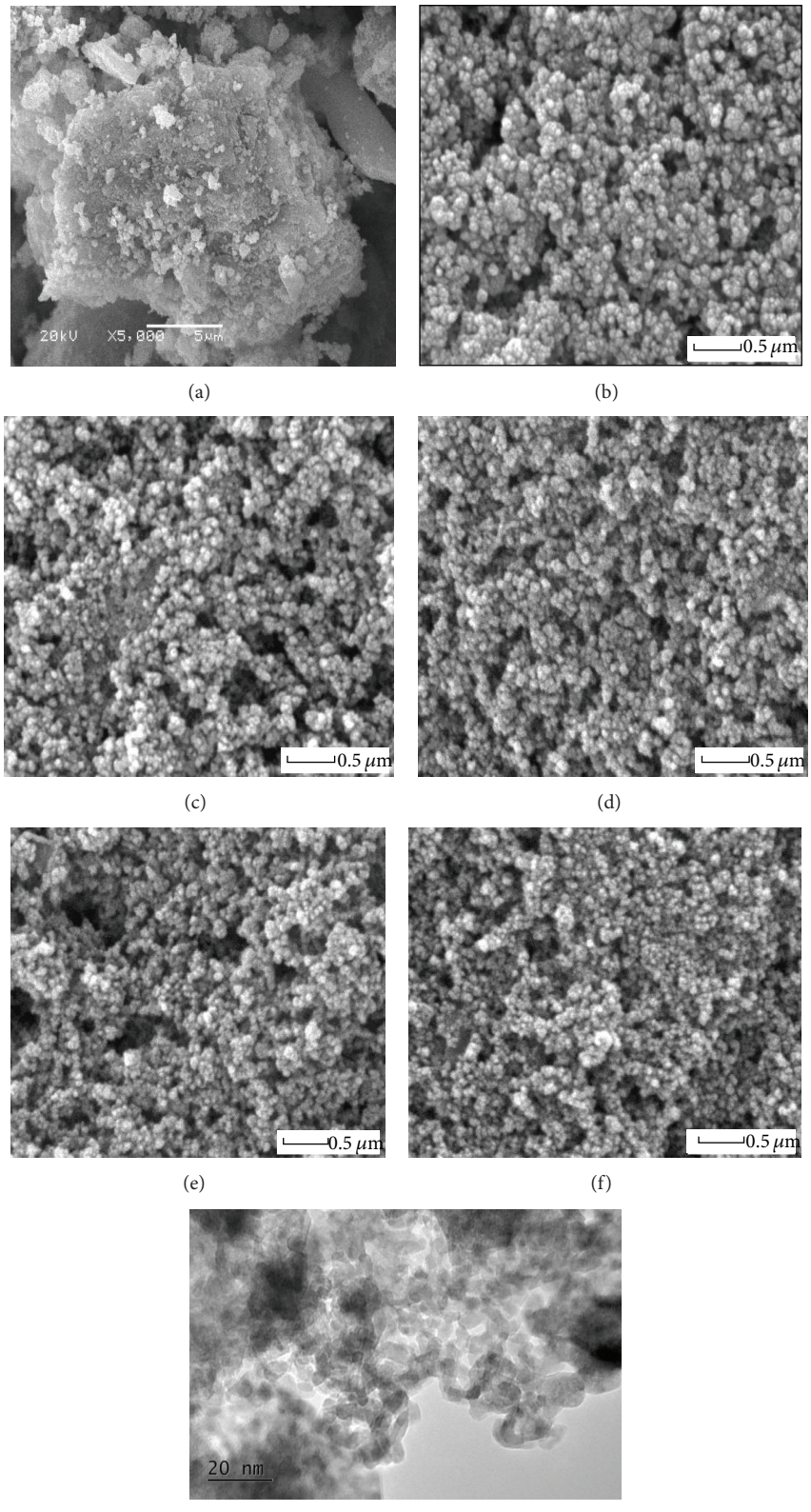

Figure 2: (a) SEM image of ZnS:Tb^{3+} nanocrystals prepared by the direct precipitation method (Tb^{3+} doping concentration, 5%), (b), (c), (d), (e), and (f) SEM images of ZnS:Tb^{3+} nanocrystals prepared by the spray precipitation method (Tb^{3+} doping concentration, 5%, 1%, 3%, 7%, and 9%, resp.), and (g) TEM image of ZnS:Tb^{3+} nanocrystals prepared by the spray precipitation method (Tb^{3+} doping concentration, 5%).

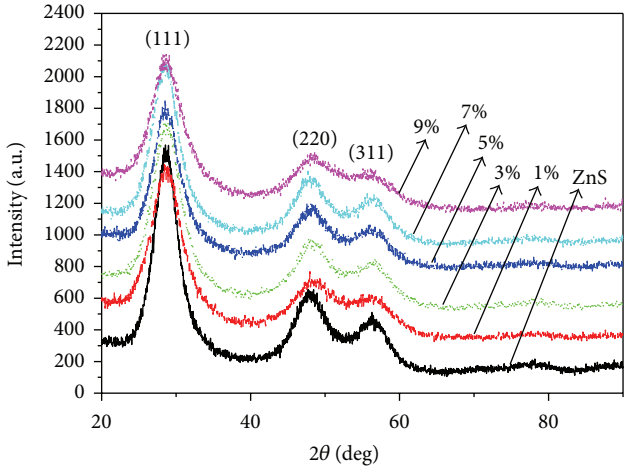

Figure 3: XRD patterns of ZnS:Tb^{3+} nanocrystals.

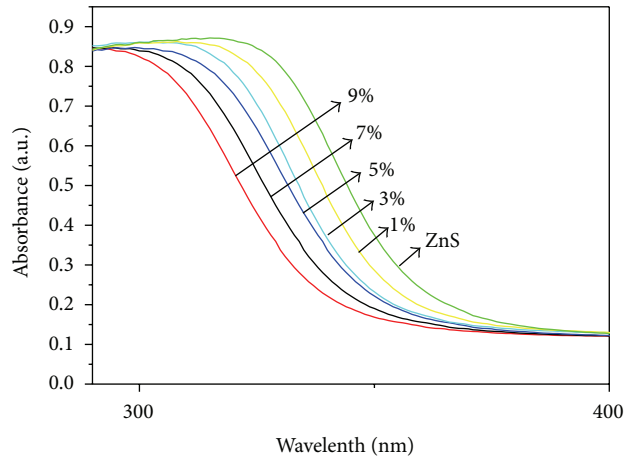

Figure 4: UV-Vis absorption spectra of ZnS:Tb^{3+} and undoped ZnS nanocrystals.

phenomena: simultaneous formation of large crystal nuclei on the droplet surface and liquid contact surface and crystal nucleus for nanocrystal gradually grew up in almost the same environment during the synthetic process of ZnS:Tb^{3+} nanocrystals which have been synthesized by spray precipitation method, but the direct precipitation nucleation has less nucleus conditions and growth environment is different each time.

The luminescence properties of the ZnS:Tb^{3+} with different doping concentrations will vary with their shapes and sizes. But the sizes and shapes of the ZnS:Tb^{3+} nanocrystals shown in Figures 2(b), 2(c), 2(d), 2(e), and 2(f) were almost identical because the nanocrystals were synthesized by the same method. So, the luminescence properties of the ZnS:Tb^{3+} nanocrystals mainly depend on the doping concentration rather than on their shapes and sizes.

The XRD patterns of different ZnS:Tb^{3+} nanocrystals and undoped ZnS nanocrystals are shown in Figure 3. The patterns reveal that the nanocrystals exhibit a zinc blende crystal structure. The three diffraction peaks observed correspond to the (111), (220), and (311) planes of face-centered cubic crystalline ZnS (JCPDS number 77-2100). Considering the size effect, the XRD peaks broadened and their widths increased as the crystals became smaller. The average sizes of the ZnS:Tb^{3+} nanocrystals calculated from the Debye-Scherrer equation were determined to be approximately 10 nm. The TEM image of ZnS:Tb^{3+} nanocrystals is shown in Figure 2(g); here, the average size of the ZnS:Tb^{3+} nanocrystals is between 8 nm and 12 nm, which agrees well with our XRD estimation. Tb^{3+} doping appeared to destroy the crystalline nature of ZnS, as can be seen from changes in the graph of the (220) and (311) crystal planes. This destruction causes lattice distortions and produces a large number of lattice defects. In addition, the spectrum-verified doping concentrations have different optical properties.

The UV-Vis absorption spectra of different ZnS:Tb^{3+} and undoped ZnS nanocrystals are shown in Figure 4. The maximum absorption wavelength range of ZnS:Tb^{3+} and undoped ZnS nanocrystals was nearly 300–400 nm. The maximum

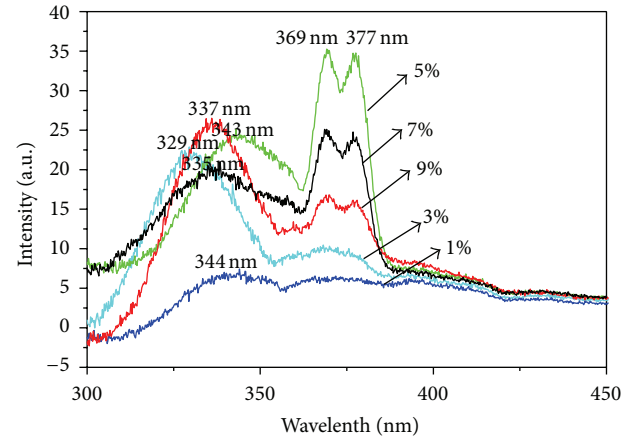

Figure 5: Excitation spectra of ZnS:Tb^{3+} nanocrystals.

absorption wavelength of ZnS:Tb^{3+} nanocrystals was shorter than that of undoped ZnS nanocrystals, and the absorption peak band of the crystals positively blueshifted with increasing concentrations of the Tb^{3+} dopant. We believe that doping with Tb^{3+} changes the crystal structure and band gap structure of semiconductor ZnS.

Figure 5 shows the excitation spectra of ZnS:Tb^{3+} nanocrystals with doping concentrations of 1%, 3%, 5%, 7%, and 9% at an emission wavelength of 545 nm. The two peaks at 369 and 377 nm are characteristic Tb^{3+} excitation peaks. The peak intensity of the ZnS:Tb^{3+} nanocrystals increased at doping concentrations of 1%, 3%, and 5% and decreased at doping concentrations of 5%, 7%, and 9%. Therefore, the peak intensity of ZnS:Tb^{3+} nanocrystals is strongest at 5% doping concentration because of lattice saturation. Red shifting of the excitation peak position of ZnS at 5% doping compared with those of crystals at 1%, 3%, 7%, and 9% doping may also be observed.

Figure 6 shows the emission spectra of ZnS:Tb^{3+} nanocrystals with doping concentrations of 1%, 3%, 5%, 7%, and 9% at an excitation wavelength of 369 nm. As all emission

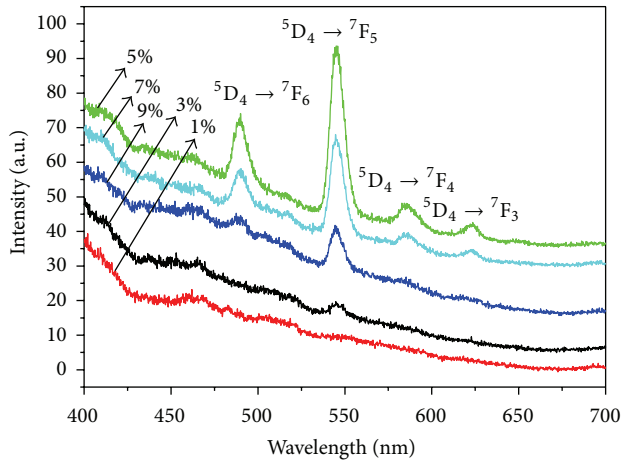

FIGURE 6: Emission spectra of ZnS:Tb^{3+} nanocrystals (λ_{exc} = 369 nm).

spectra were recorded under the same conditions, the relative intensities of peaks obtained are directly comparable. The PL spectral features of lower doping concentrations are nearly identical, although their PL intensities are weak. The PL spectral features of higher doping concentrations are nearly identical, although their PL intensities vary significantly. The PL intensities were strongest at 5% doping concentration. The PL peak at ~545 nm was strongest in the investigated range, which indicates that ZnS:Tb^{3+} nanocrystals have strong green light emission. The intense green emission of ZnS:Tb^{3+} nanocrystals by F4500 excitation (at 369 nm) is visible to the naked eye. The strongest emission peak corresponds to the $^5D_4 \rightarrow {}^7F_5$ (at ~545 nm) transition of Tb^{3+} ions. Other PL peaks identified correspond to the following transitions: $^5D_4 \rightarrow {}^7F_6$ (at ~489 nm), $^5D_4 \rightarrow {}^7F_4$ (at ~594 nm), and $^5D_4 \rightarrow {}^7F_3$ (at ~625 nm).

Our experimental results show that the increase in doping concentration has important effects on the structure and luminescence properties of the resultant nanocrystals. As shown in Figure 6, the luminescence intensity of 5 mol% ZnS:Tb^{3+} nanocrystals was stronger than that of any other ZnS sample under excitation at 369 nm. The holes and electrons in ZnS:Tb^{3+} nanocrystals recombined to form excitons on the ZnS host, and the exciton energy then transferred to the resonance levels of Tb^{3+} ions to achieve the characteristic emissions of Tb^{3+}. This energy is most efficiently transferred in 5 mol% ZnS:Tb^{3+} nanocrystals because 5 mol% Tb^{3+} has an adequate amount of saturated interspace in the whole body-centered cubic ZnS crystalline lattice (Figure 6).

4. Conclusions

In summary, we have successfully synthesized monodispersed ZnS:Tb^{3+} nanocrystals with diameters of approximately 10 nm by spray precipitation with SRB culture at room temperature. The ZnS:Tb^{3+} nanocrystals exhibited a zinc blende crystal structure. The main peak position of the absorption spectra positively blueshifted with increasing concentration of Tb^{3+} dopant. The luminescence intensity of 5 mol% ZnS:Tb^{3+} nanocrystals was the strongest among all other ZnS products obtained. Four emission peaks located at 489 nm ($^5D_4 \rightarrow {}^7F_6$), 545 nm ($^5D_4 \rightarrow {}^7F_5$), 594 nm ($^5D_4 \rightarrow {}^7F_4$), and 625 nm ($^5D_4 \rightarrow {}^7F_3$) at 369 nm excitation were observed. Of these peaks, the emission peak intensity was strongest at 545 nm ($^5D_4 \rightarrow {}^7F_5$). Hence, the 5 mol% ZnS:Tb^{3+} nanocrystals can be used as green fluorescent materials. Nanocrystals have potential applications in photoelectronic devices and biomarkers. We believe that many types of Re ion-doped ZnS nanocrystals can be synthesized by the spray precipitation method.

Conflict of Interests

The authors declare that there is no conflict of interests regarding the publication of this paper.

Acknowledgments

This work was supported by the Liaoning BaiQianWan Talents Program (2012921052) and Chinese National Programs for High Technology Research and Development (2011AA09070305).

References

[1] R. Maity, U. N. Maiti, M. K. Mitra, and K. K. Chattopadhyay, "Synthesis and optical characterization of polymer-capped nanocrystalline ZnS thin films by chemical process," *Physica E: Low-Dimensional Systems and Nanostructures*, vol. 33, no. 1, pp. 104–109, 2006.

[2] S. J. Yun, S. Dey, and K.-S. Nam, "Zinc sulfide and terbium-doped zinc sulfide films grown by traveling wave reactor atomic layer epitaxy," *Journal of the Korean Physical Society*, vol. 33, no. 2, pp. S454–S457, 1998.

[3] S. Zeng, M.-K. Tsang, C.-F. Chan, K.-L. Wong, B. Fei, and J. Hao, "Dual-modal fluorescent/magnetic bioprobes based on small sized upconversion nanoparticles of amine-functionalized BaGdF 5:Yb/Er," *Nanoscale*, vol. 4, no. 16, pp. 5118–5124, 2012.

[4] B. R. Judd, "Optical absorption intensities of rare-earth ions," *Physical Review*, vol. 127, no. 3, pp. 750–761, 1962.

[5] S. J. Zeng, G. Z. Ren, and C. F. Xu, "Intense blue photo luminescence of Tm^{3+}/Yb^{3+} co-doped single-crystalline hexagonal phase $NaYF_4$ nanorods," *Journal of Alloys and Compounds*, vol. 509, no. 5, pp. 2540–2543, 2011.

[6] R. N. Bhargava, D. Gallagher, X. Hong, and A. Nurmikko, "Optical properties of manganese-doped nanocrystals of ZnS," *Physical Review Letters*, vol. 72, no. 3, pp. 416–419, 1994.

[7] R. N. Bhargava, D. Gallagher, and T. Welker, "Doped nanocrystals of semiconductors—a new class of luminescent materials," *Journal of Luminescence*, vol. 60-61, pp. 275–280, 1994.

[8] R. S. Kane, R. E. Cohen, and R. Silbey, "Synthesis of doped ZnS nanoclusters within block copolymer nanoreactors," *Chemistry of Materials*, vol. 11, no. 1, pp. 90–93, 1999.

[9] S. J. Xu, S. J. Chua, B. Liu, L. M. Gan, C. H. Chew, and G. Q. Xu, "Luminescence characteristics of impurities-activated ZnS nanocrystals prepared in microemulsion with hydrothermal treatment," *Applied Physics Letters*, vol. 73, no. 4, pp. 478–480, 1998.

[10] T. Kezuka, M. Konishi, T. Isobe, and M. Senna, "Preparation and properties of nanocrystalline ZnS:Mn-polymer composite films," *Journal of Luminescence*, vol. 87, pp. 418–420, 2000.

[11] S. Maiti, H. Y. Chen, Y. Park, and D. H. Son, "Evidence for the ligand-assisted energy transfer from trapped exciton to dopant in Mn-doped CdS/ZnS semiconductor nanocrystals," *The Journal of Physical Chemistry C*, vol. 118, no. 31, pp. 18226–18232, 2014.

[12] T. Igarashi, T. Isobe, and M. Senna, "EPR study of Mn^{2+} electronic states for the nanosized ZnS:Mn powder modified by acrylic acid," *Physical Review B*, vol. 56, no. 11, pp. 6444–6445, 1997.

[13] T. Kubo, T. Isobe, and M. Senna, "Enhancement of photoluminescence of ZnS:Mn nanocrystals modified by surfactants with phosphate or carboxyl groups via a reverse micelle method," *Journal of Luminescence*, vol. 99, no. 1, pp. 39–45, 2002.

[14] M. Tanaka, J. Qi, and Y. Masumoto, "Comparison of energy levels of Mn^{2+} in nanosized- and bulk-ZnS crystals," *Journal of Luminescence*, vol. 87–89, pp. 472–474, 2000.

[15] H. F. Wang, Y. Y. Wu, and X. P. Yan, "Room-temperature phosphorescent discrimination of catechol from resorcinol and hydroquinone based on sodium tripolyphosphate capped Mn-doped ZnS quantum dots," *Analytical Chemistry*, vol. 85, no. 3, pp. 1920–1925, 2013.

[16] B. Xia, I. W. Lenggoro, and K. Okuyama, "Synthesis and photoluminescence of spherical ZnS: Mn^{2+} particles," *Chemistry of Materials*, vol. 14, no. 12, pp. 4969–4974, 2002.

[17] M. Ihara, T. Igarashi, T. Kusunoki, and K. Ohno, "Preparation and characterization of rare earth activators doped nanocrystal phosphors," *Journal of the Electrochemical Society*, vol. 147, no. 6, pp. 2355–2357, 2000.

[18] P. Yang, M. Lü, D. Xü, D. Yuan, and G. Zhou, "Photoluminescence properties of ZnS nanoparticles co-doped with Pb^{2+} and Cu^{2+}," *Chemical Physics Letters*, vol. 336, no. 1-2, pp. 76–80, 2001.

[19] D. C. Krupka, "Hot-electron impact excitation of Tb^{3+} luminescence in ZnS: Tb^{3+} thin films," *Journal of Applied Physics*, vol. 43, no. 2, pp. 476–481, 1972.

[20] A. A. Bol, R. van Beek, and A. Meijerink, "On the incorporation of trivalent rare earth ions in II-VI semiconductor nanocrystals," *Chemistry of Materials*, vol. 14, no. 3, pp. 1121–1126, 2002.

[21] L. Sun, C. Yan, C. Liu, C. Liao, D. Li, and J. Yu, "Study of the optical properties of Eu^{3+}-doped ZnS nanocrystals," *Journal of Alloys and Compounds*, vol. 275–277, pp. 234–237, 1998.

[22] K. Wiatek, M. Godlewski, and D. Hommel, "Deep europium-bound exciton in a ZnS lattice," *Physical Review B*, vol. 42, no. 6, pp. 3628–3633, 1990.

[23] S. C. Qu, W. H. Zhou, F. Q. Liu et al., "Photoluminescence properties of Eu^{3+}-doped ZnS nanocrystals prepared in a water/methanol solution," *Applied Physics Letters*, vol. 80, no. 19, pp. 3605–3607, 2002.

[24] D. D. Papakonstantinou, J. Huang, and P. Lianos, "Photoluminescence of ZnS nanoparticles doped with europium ions in a polymer matrix," *Journal of Materials Science Letters*, vol. 17, no. 18, pp. 1571–1573, 1998.

[25] W. Chen, J.-O. Malm, V. Zwiller et al., "Energy structure and fluorescence of Eu^{2+} in ZnS:Eu nanoparticles," *Physical Review B: Condensed Matter and Materials Physics*, vol. 61, no. 16, pp. 11021–11024, 2000.

[26] J. H. Niu, R. N. Hua, W. L. Li, M. T. Li, and T. Z. Yu, "Electroluminescent properties of a device based on terbium-doped ZnS nanocrystals," *Journal of Physics D: Applied Physics*, vol. 39, no. 11, pp. 2357–2360, 2006.